Liquid Crystals, Vol. 34, No. 12, December 2007, 1433–1441

Taylor & Francis
Taylor & Francis Group

Optical anisotropy and liquid-crystal alignment properties of rubbed polyimide layers

FUZI YANG*†‡, G. ZORINIANTS‡, LIZHEN RUAN‡ and J.R. SAMBLES‡

†Chemistry Department, Tsinghua University, Beijing 100084, China
‡Electromagnetic Materials, School of Physics, University of Exeter, Exeter EX4 4QL, UK

(*Received 2 July 2007; accepted 8 October 2007*)

The relation between the optical anisotropy of rubbed polyimide layers and the rubbing process is investigated using the recently developed polarization-conversion guided mode technique. Results indicate that the effective optical anisotropy of the polyimide layers may be substantially changed by the rubbing process, although this does not significantly influence the ability of the polyimide layers to align liquid crystals.

1. Introduction

The alignment of the liquid-crystal director is a key issue as regards the function of liquid-crystal displays (LCDs). Over the last few decades a variety of aligning materials and procedures have been employed to treat the inside surfaces of the glass plates which confine the liquid crystal to realize this alignment. These include obliquely evaporated SiOx films [1, 2], mechanically rubbed polyimide layers [3], photo-aligned light sensitive polymers [4], Langmuir–Blodgett films [5], lithographically micro-patterned polymers [6], nanopatterned surfaces using an atomic force microscope (AFM) or ion-beam etching surfaces [7], etc. Owing to their low cost and the ease with which large areas may be coated with high-quality uniform films, rubbed polyimide layers are by far the most commonly used alignment method in commercial devices. This is despite a number of problems associated with the rubbing operation, e.g., static charging, surface debris created on the layers and degradation of the rubbing fabric, etc. The procedure for producing the alignment layer is that a thin layer of long-chain polymer, such as polyimide, is first spread onto the substrate surface and then, after baking at a high temperature, buffed using a suitable fabric. There are two consequences arising from this rubbing process, one is the creation of microgrooves and the other is a reordering of the long-chain organic molecules on the rubbed surface. In principle, both of these can introduce optical anisotropy on the surfaces and both may act to align the liquid-crystal director. Thus, determining the optical anisotropy of the rubbed polyimide layer should give information about the rubbing process and possibly the alignment ability of the surfaces.

Recently, reflection anisotropy spectroscopy (RAS) has been developed and used extensively in this type of surface study [8–10]. RAS is an optical spectroscopic technique used to measure the optical anisotropy of surfaces and thin layers using normal incidence reflection: in principle, it is polarization-conversion reflection ellipsometry at normal incidence. Some studies of rubbed polyimide liquid-crystal alignment layers using the RAS technique have been published [11, 12]. In these articles the authors have investigated the relationship between the surface topography, the dielectric properties of the mechanically rubbed thin polymer layers and the optical anisotropy deduced from the RAS data, and suggested the possibility that the RAS technique may have a role as a new process control tool in liquid-crystal device fabrication.

In general, RAS is used to explore electronic surface states in semiconductors and the arrangement used is an optical beam fixed at normal incidence with the optical wavelength (energy) being scanned. This means that either expensive tunable lasers or a monochromator are required. Furthermore, because of the lack of incident angle (in-plane momentum) scanning, information about the distribution of the anisotropy within the thin surface layers, which may be vital for the study of the relationship between the rubbing-induced anisotropy and the aligning ability of the thin layers, may be unobtainable. It would be of substantial advantage to be able to use one wavelength while scanning the angle (in-plane momentum) to give similar information to that provided by the RAS technique.

*Corresponding author. Email: f.yang@exeter.ac.uk

Liquid Crystals
ISSN 0267-8292 print/ISSN 1366-5855 online © 2007 Taylor & Francis
http://www.tandf.co.uk/journals
DOI: 10.1080/02678290701732970

In this study, the very recently developed polarization-conversion guided mode (PCGM) technique [13] has been used to explore the small optical anisotropy of very thin rubbed polyimide layers. Using the PCGM geometry with the prism coupler connected by index-matching fluid to the sample cell, the sample rotation angle can be easily varied. This then allows even more detailed investigation of the optical anisotropy within the rubbed polyimide layer and is particularly useful for determining the direction of an optical axis, if it exists, of the layer.

Several rubbed polyimide samples with the same polyimide coating and different amounts of rubbing have been investigated by the PCGM technique.

2. The PCGM technique

The sample geometry of the PCGM technique [13] is shown in figure 1, with details of the sample cell in the inset. A standard index prism coupler (n=1.517 at 632.8 nm) is contacted to the top glass plate of the sample cell with an index-matching fluid, allowing the sample rotation angle, Φ, to be freely varied relative to the incident plane on the prism bottom surface. The sample waveguide cell is composed of two low-index glass plates with Mylar spacers (thickness of about 15 μm) to give an air gap. The thin layer to be characterized and a thick gold coating are on the inner surfaces of the top and bottom plates, respectively. The thick gold coating is simply a good mirror to enhance the p to s conversion guided mode signals. This whole sample assembly is mounted on a computer controlled θ–2θ rotation stage [14] and a monochromatic (633 nm) p-polarized incoming beam from a He–Ne laser enters the geometry from one prism face and exits through the other face to the detector having an s-polarizer in front of it. Thus, the p to s conversion signal is recorded while varying the external incident angle of the beam.

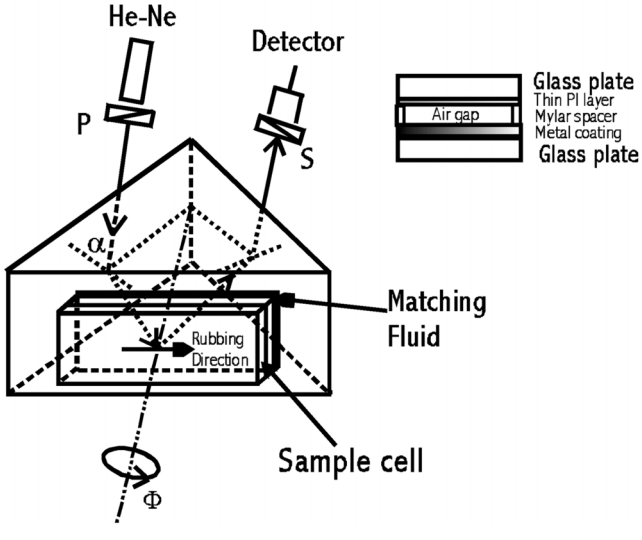

Figure 1. The geometry of the PCGM technique. The inset is the sample cell.

As the layer to be detected may be quite thin (<20 nm) and the optical anisotropy introduced by rubbing may be quite small, $\Delta n \sim 0.1$–0.2 (see [11, 12]), then the p to s conversion signals recorded from the experimental work are expected to be of the order of 10^{-4} to 10^{-5}. Thus, the resolution of the PCGM technique should be at least of the order of 10^{-5} to extract the p to s conversion signals created by the thin layers. This means that other sources of apparent p to s conversion have to be minimized. Thus, care has to be taken with regards to setting the polarization of the incoming beam relative to the incident faces of the sample, the parallelism between the prism bottom surface and the top surface of the sample cell, and also in establishing carefully that there is no pressure induced birefringence in the prism and sample cell [13]. With such care, and taking into account from modelling that p to s conversion signals arising from these other sources have a different angular dependence to that from the thin sample, then the requisite resolution may be achieved.

3. Experiment

Two sets of samples, both sets being five glass plates each with a rubbed polyimide layer, AL 1254 (JSR Corporation, Japan), have been studied. All of the sample layers are made by exactly the same spin coating and baking procedure. In addition the rubbing conditions are the same for each sample except that the number of 'rubs' are one, two, three, four and five for the five samples of the two sets. The time gap between each rub is at least a minute for every sample.

To help characterize the sample morphologies surface topography images for all of the rubbed layers have been taken using an AFM (NT-MDT). From these AFM images the microgroove profiles, their mean period and mean thickness are obtained. The whole polyimide layer thickness can also be determined.

Then air-gap sample cells, as described above, have been made for the PCGM measurements. For all of the sample cells the p to s conversion signals are recorded as a function of the external incidence angle, α, for three sample rotation angles, Φ, between the rubbing direction and the incident plane, 0°, 45° and 90° (see Figure 1).

Then, finally, twisted nematic (TN) liquid-crystal cells are made using these characterized aligning layers together with suitable Mylar spacers, the nematic liquid

crystal (E7; Merck-BDH) and a second rubbed polyimide coated glass slide from an industrial product line. These cells were then checked for the quality of alignment using crossed polarization microscopy (CPM; Solver Pro-M) as well as sets of p to s conversion data taken using the standard fully-leaky guided mode (FLGM) technique [14].

4. Discussion

Five AFM images for the layers of the first sample set are shown in figures 2 (a)–(e). From these images one can clearly see that grooves having the same direction as the rubbing direction appear on every sample surface. Five sets of p to s conversion signals, corresponding to the above five samples are shown in figures 3 (a)–(e). From figures 3 (a)–(e) it is apparent that the optical p to s conversion signal varies significantly with the number of 'rubs'. Also from Figure 3 note that the p to s conversion signals for $\Phi=45^\circ$ are much higher than the signals obtained at $\Phi=0^\circ$ and 90° for each samples, indicating that the layer is at least uniaxial with the effective optical axis along the rubbing direction for the five samples of this first set. However, is this from the molecular structure (alignment of the molecules) or is it simply form-birefringence owing to the microgrooves? From the AFM images the mean period and mean depth of the microgrooves can be extracted: typical

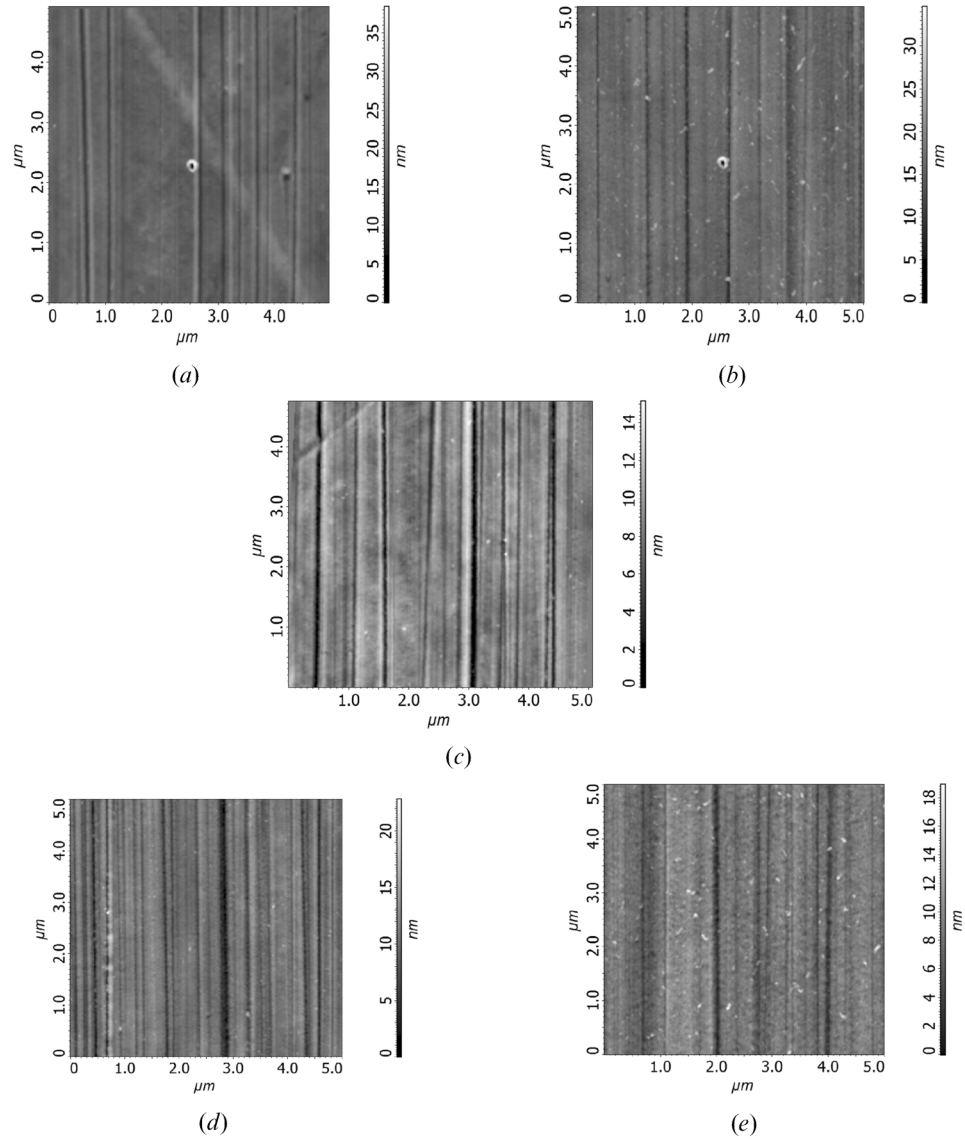

Figure 2. AFM images of the rubbed polyimide layers of the first set of samples. The number of rubs are (a) one, (b) two, (c) three, (d) four and (e) five.

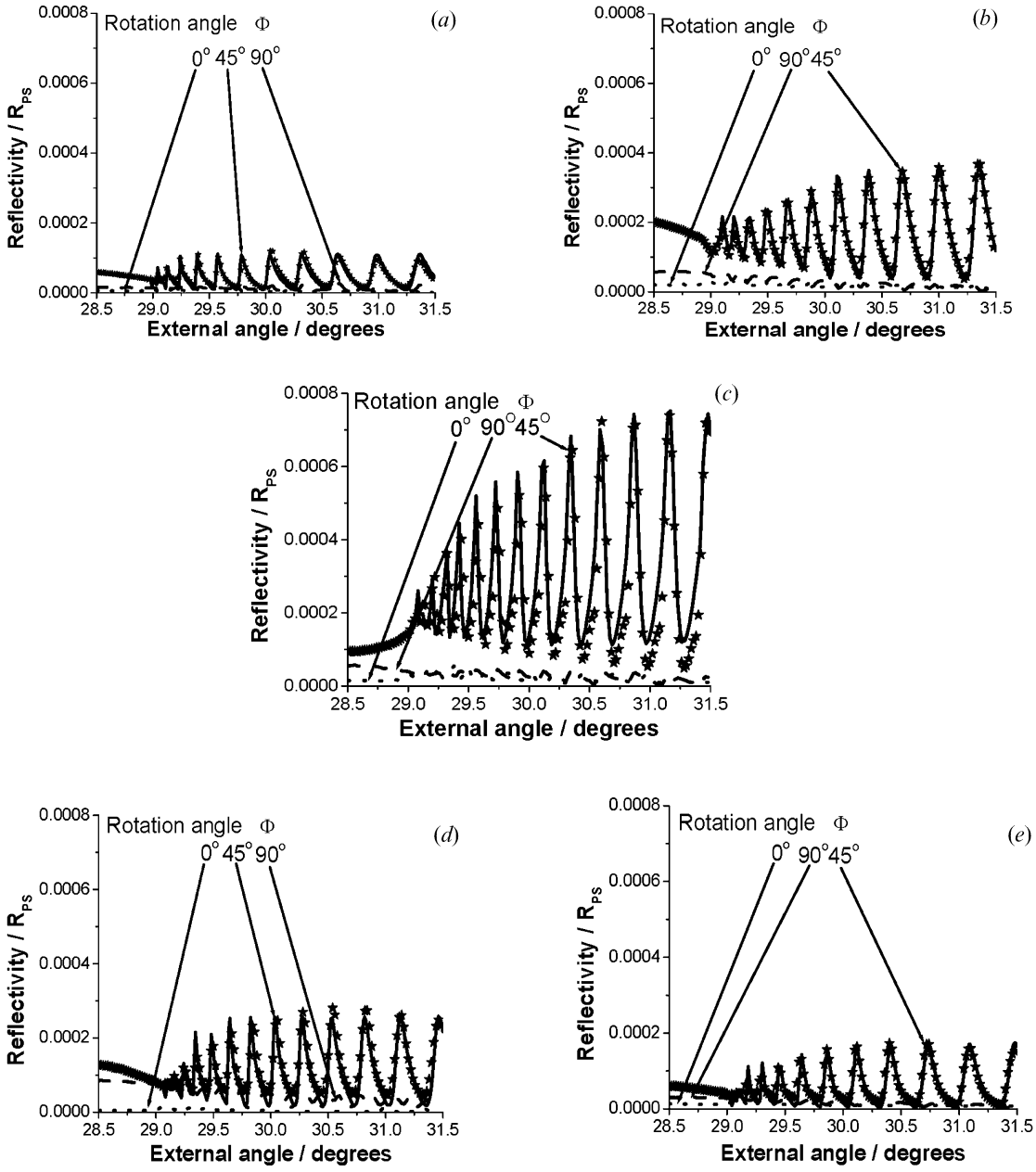

Figure 3. Experimental R_{ps} signals (symbol, dot and dash lines) for the first set of samples against external incident angle for three different rotation angles, $\Phi=0^\circ$, 45° and 90°. The number of rubs are (a) one, (b) two, (c) three, (d) four and (e) five. The solid lines are theoretical modelling. The optical permittivity for the gold film is $\varepsilon_{Au}=-10.50+i1.450$.

examples of 2D and 3D diagrams for the samples rubbed one and three times are shown in figure 4. It is clear that the mean period and depth are of the order of 100 and 10 nm, respectively. This means that, with the wavelength of the radiation used (632.8 nm) being much larger than the mean period and depth mentioned above, the form-birefringence from the grooves is expected to be very weak and may be ignored, as for a 60°-evaporated SiOx aligning layer [13]. Also, to determine the total thickness of the polyimide layer, the AFM tip has been pushed hard to pierce the polyimide layer and to touch the substrate glass surface making a hole image which may be seen in figures 4 (a) and (b). From figure 4 (b) it is apparent that the polyimide layer has a total thickness of about 22.0 nm with a mean rubbing depth of only about 7.0 nm. This indicates that the rubbed polyimide layer should be modelled optically using at least a two-layer model as mentioned in earlier

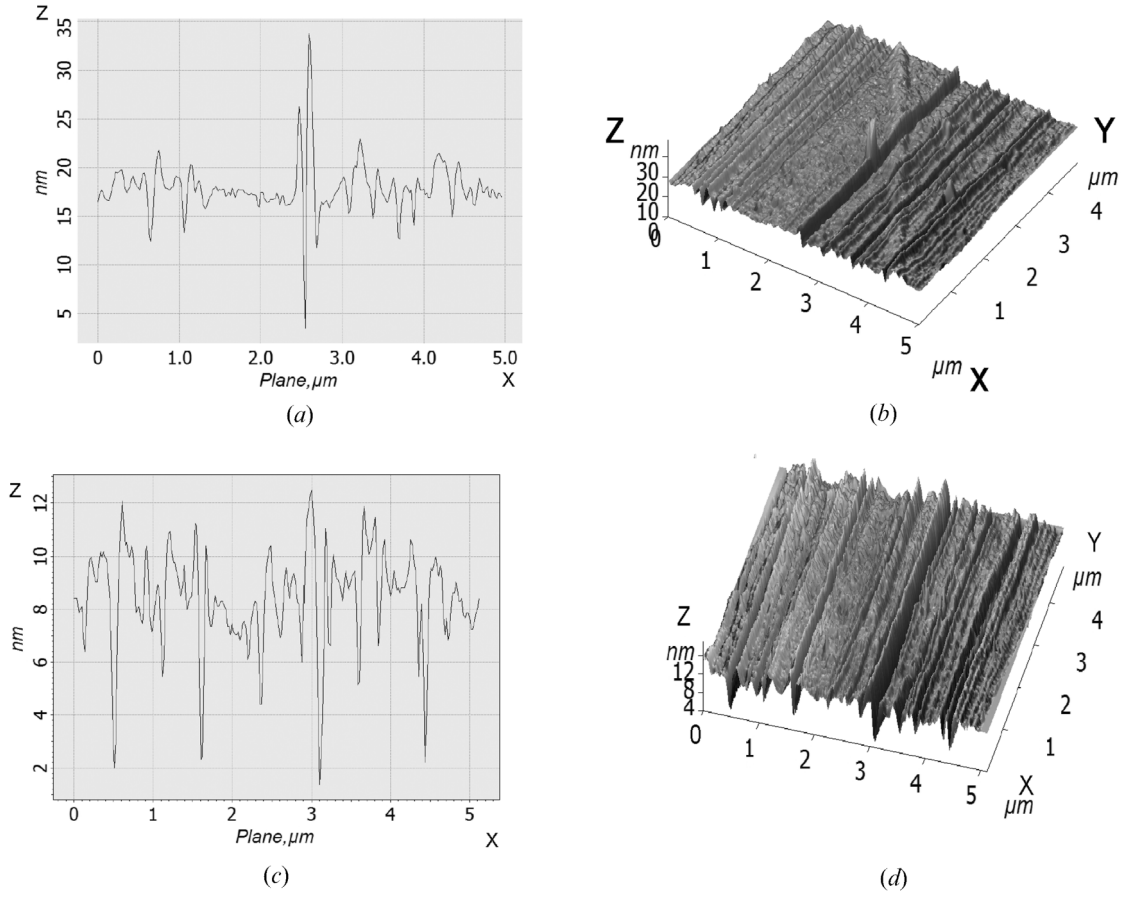

Figure 4. The 2D profiles and 3D images extracted from the AFM pictures for polyimide layers of the first set of samples rubbed one and three times.

literature [15]. This is established by measuring the mean depth of the grooves and setting this as the rubbed layer thickness (of course, this may not be quite correct, but with a simple two-layer model it is a reasonable approximation), then regarding only this thickness of the layer as optically anisotropic. Then with a mean optical index of 1.6350 (permittivity of 2.6720) for the isotropic region the effective anisotropy, Δn, for each rubbed polyimide layer is obtained by fitting a two-layer model to the p to s conversion at $\Phi=45^\circ$. The Berreman 4x4 matrix model has been used in the fitting process. This model takes into account the multi-reflections due to all the interfaces in the optical system. The fitting results are shown in figure 3 as solid lines and the relation between the mean rubbed thickness and the effective optical anisotropy, Δn, of the rubbed polyimide layers with rubbing times are shown in figures 5 (a) and (b), respectively. From figure 5 it is apparent that the rubbed thickness and the degree of the reordering of the polyimide molecules increases with the first few rubs from one to three, but then decreases for further rubs from three to five. This is confirmed by the behaviour of the ratio between the amplitudes of the minimum, for $\Phi=0^\circ$ and/or 90°, and maximum, for $\Phi=45^\circ$, p to s conversion signal. These ratios diminish from one to three rubs then grow for three to five rubs. This phenomenon suggests that the degree of order of the reordered molecules increases for one to three rubs and then decreases for subsequent rubs.

However, the real situation is not as simple as indicated above. For the second set of samples the behaviour of the p to s conversion signals for one and two rubs are similar to the first set of samples, but change dramatically for the third and fourth rubs. AFM images and p to s conversion signals for the sample from the second set rubbed three times are shown in figures 6 (a) and (d), respectively. It is apparent that while the grooves still lie along the rubbing direction and the 2D/3D topographies are similar to the earlier set of samples, as shown in figures 6 (a)–(c), the effective optical axis is twisted about 45° away from the rubbing direction, because the p to s conversion signals at $\Phi=0^\circ$ and 90° are now much stronger than the signal at $\Phi=45^\circ$. Repeating the procedure used for the first set,

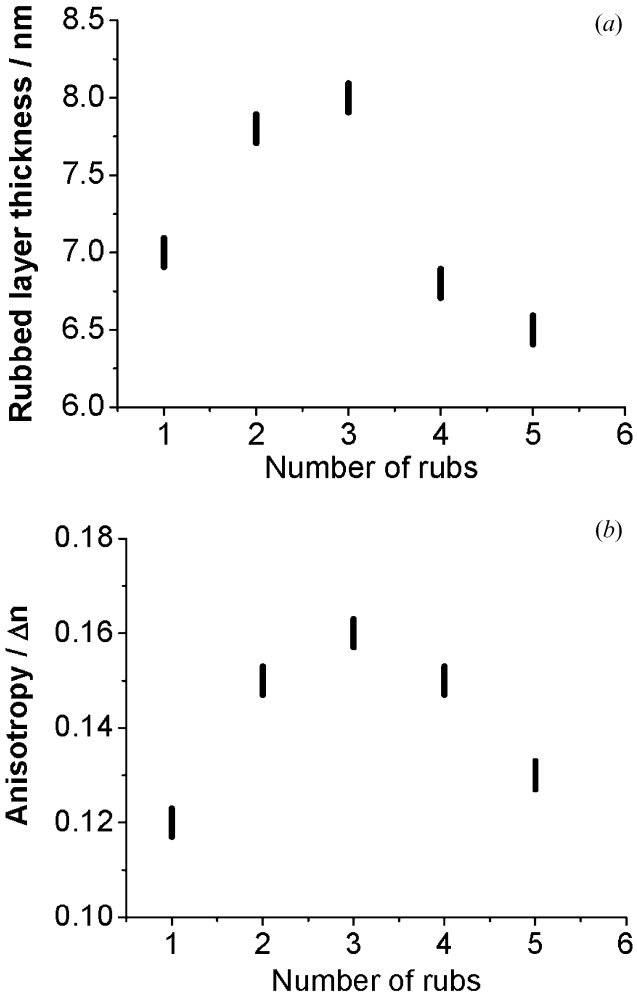

Figure 5. The mean rubbed thickness and the optical anisotropy, Δn, of the rubbed layers against number of rubs for the first set of samples.

taking the mean depth of the rubbed layer from the AFM images (figure 6 (b)) to be about 8.0 nm, the model two-layer fitting results are also shown in figure 6 (d) as solid lines for $\Phi=0^\circ$ and 90° with an optical anisotropy of $\Delta n=0.17$ and the optic axis rotated to $\sim 45^\circ$ away from the rubbing direction. This means that for some reason the induced director within the polyimide layer has been altered by the number of rubs. The p to s conversion signals for the layer of the second sample set rubbed four times are weaker than the signals from the sample rubbed three times showing once again the disorder introduced by more rubbing. The p to s conversion results for the layer of the second set of samples rubbed five times is even weaker.

Hirosawa [15] has reported that the tilt angle of the effective optical axis of the rubbed polyimide layer may be changed by about 30–40° by annealing treatments with higher temperatures, i.e. reorientation of the polyimide molecule director may be influenced by different annealing treatments. However, to the best of our knowledge this is the first report showing that the reorientation of the rubbed polyimide molecular director, the twist angle of the effective optic axis, depends on the number of rubs. The heating effect from the rubbing process may soften the polymer allowing the surface molecular order to vary with rubbing. However, why the symmetry is broken so that the optic axis appears at 45° to the rubbing direction is a mystery.

We have obtained very similar results for several different positions on these two interesting samples and almost exactly the same results have been obtained. Note also that the sample holder has been designed so that almost no pressure is applied to the sample cell avoiding any stress-induced birefringence. In addition an empty cell with no rubbed PI layers has also been checked to establish that there are no effects due to birefringence of the glass plates. However, there may of course still be some other extra effects which introduce such very weak p-s conversion signals which we have not taken into account. From the above results it seems that there is no simple and straightforward relation between the optical anisotropy and the number of rubs. Of course, the induced optical anisotropy will be dependent on the detailed procedures: the type of polymer, the spinning and baking process, the rubbing strength, etc. The above results may not be exactly repeatable; however, they very clearly show a surprising variability of molecular order and, even more startlingly, axial direction.

It is interesting to see how the various samples align liquid crystals, in particular, the sample from the second set rubbed three times. To do this each sample has been used in the fabrication of a TN cell, the other aligning plate having a rubbed polyamide layer made in an industry product line. Typical images from CPM as well as p to s conversion reflectivity signals from the standard FLGM technique for the layers of the two sample sets rubbed three times with both rubbing directions being 45° away from the incident plane are shown in figures 7 (a)–(d). From figures 7 (a) and (c) the uniformity of the CPM photos show that well-aligned TN structures have been realized. Furthermore, the standard TN-type p to s conversion reflectivity signals (star symbols) and theoretical fittings (solid lines) in figures 7 (b) and (d) show that mono-domains have been achieved for the two cells, even though the rubbed polyimide layers gave very different optical p to s conversion signals. For all of the remaining cells fabricated from the other samples, similar CPM and FLGM results are also obtained even though the optical

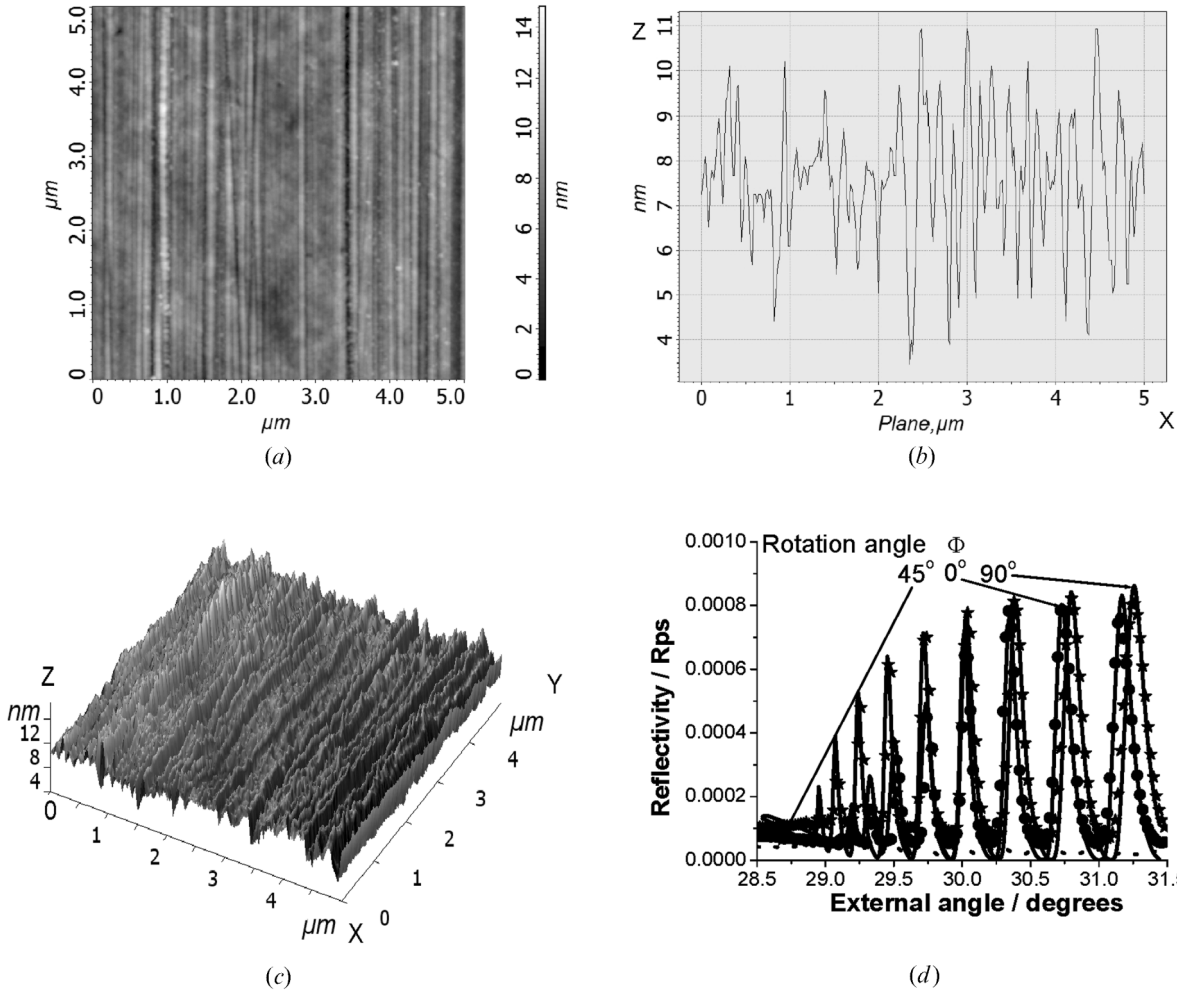

Figure 6. (a) AFM image for the layer of the second set of samples rubbed three times. Also shown are (b) the 2D profiles and (c) 3D images of the rubbed layer. (d) The R_{ps} signals (symbols and dashed line) for the layer rubbed three times. The solid lines are theoretical fits with optical permittivity for the gold film of $\varepsilon_{Au}=-10.50+i1.450$.

anisotropy of the polyimide layers are significantly different. This of course suggests that alignment is primarily via the microgrooves and not molecular in character for these particular aligning layers.

5. Conclusions

The PCGM technique [13] is a powerful tool for exploring very weak optical anisotropy of thin surface layers. In this study the technique has been used to determine the optical anisotropies of rubbed polyimide layers with different amounts of rubbing. AFM has been used to help characterize the layers while CPM and FLGM techniques have been used to investigate the relation between the optical anisotropy and the ability of the aligning layer to align the liquid crystals. From the experimental results several conclusions may be obtained.

1. The rubbing process creates two effects in the polyimide layers: the production of unidirectional microgroove structures and the creation of optical anisotropy introduced by reordering of the long-chain polyimide molecules.
2. The liquid-crystal director alignment is mainly caused by the microgroove structures.
3. Optical anisotropy caused by the form-birefringence arising from the grooves is very weak and undetectable by the techniques used here.
4. The optical anisotropy arising from the reordered long-chain polyimide molecules is of the order of 0.17.
5. The relation between this anisotropy and the rubbing process is quite complex with the anisotropy, the thickness of the disturbed layer, the degree of molecular disorder and even the direction of the effective optical axis being varied by the

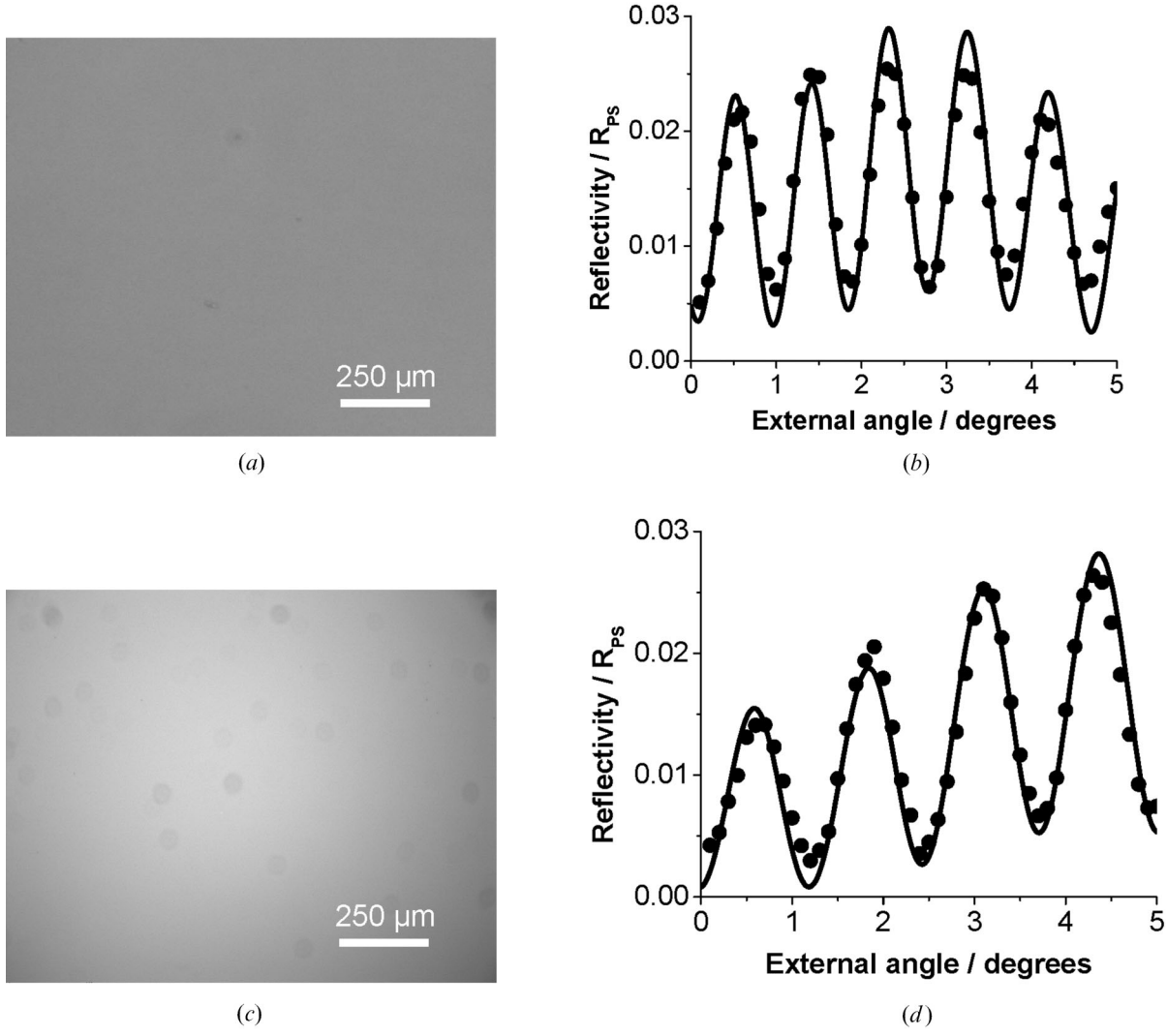

Figure 7. (a) CPM image and (b) R_{ps} signal (•) from the FLGM technique for a TN liquid crystal cell made from the layer of the first set of samples rubbed three times. (c) CPM image and (d) R_{ps} signal (•) from the FLGM technique for a TN liquid crystal cell made from the layer of the second set of samples rubbed three times. The solid lines in (b) and (d) are theoretical fitting results. The parameters of the liquid crystal for the fits are $\varepsilon_{xx}=\varepsilon_{yy}=2.3265+i0.0002$, $\varepsilon_{zz}=3.0230+i0.0002$ with thicknesses $d_{LC}=26.90$ and 19.30 μm for the cases (b) and (d), respectively.

rubbing processes. The details of this variation may well depend on the fabrication procedure used for the polyimide layers, i.e. the spinning and baking, and the rubbing strength and number of rubs.

6. As the liquid-crystal director is aligned primarily by the microgroove structures, as for obliquely evaporated SiOx thin films [13], and not by the variable anisotropy of the rubbed polyimide layers, then characterizing the optical anisotropy of the rubbed polyimide layer may not be a good method for controlling and monitoring the aligning ability of the rubbing processes using either RAS [11, 12] or PCGM [13]. However, as a new powerful surface exploration tool the PCGM technique may be employed to study non-invasively a wide range of thin films such as bio- and chemical coatings etc.

Acknowledgements

We acknowledge support by the EPSRC and thank the University of Exeter for granting the position of visiting Professor to Professor Fuzi Yang.

References

[1] J.L. Janning. *Appl. Phys. Lett.*, **21**, 173–174 (1972).
[2] J. Cognard. *Mol. Cryst. Liq. Cryst. Suppl.*, **1**, 1–77 (1982).
[3] B. Bahadur. *Mol. Cryst. Liq. Cryst.*, **109**, 3–93 (1984).
[4] S.C. Jain, H.-S. Kitzerow. *Appl. Phys. Lett.*, **64**, 2946–2948 (1994).
[5] G. Barbero, A.G. Petrov. *J. Phys. Condens. Matter.*, **6**, 2291–2306 (1994).
[6] A.J. Pidduck, S.D. Haslam, G.P. Bryan-Broan, R. Bannister, I.D. Kitely. *Appl. Phys. Lett.*, **71**, 2907–2909 (1997).
[7] P. Chaudhari, et al. *Nature*, **411**, 56–59 (2001).
[8] P. Weightman, D.S. Martin, R.J. Cole, T. Farrell. *Rep. Prog. Phys.*, **68**, 1251–1341 (2005).
[9] C. Di Natale, C. Goletti, R. Paolesse, F. Della Sala, M. Drago, P. Chiaradia, P. Lugli and A. D'Amico. *Phys. Lett.*, **77**, 3164–3166 (2000).
[10] L.D. Sun, M. Hohage, P. Zeppenfeld, S. Berkebile, G. Koller, F.P. Netzer and M.G. Ramsey. *Appl. Phys. Lett.*, **88**, 121913 (2006).
[11] B.F. Macdonald and R.J. Cole. *J. Phys. D*, **36**, 142–145 (2003).
[12] B.F. Macdonald, W. Zheng and R.J. Cole. *J. Appl. Phys.*, **93**, 4442–4446 (2003).
[13] Fuzi Yang, Lizhen Ruang and J.R. Sambles. *Optics Express*, **15**, 11234–11240 (2007).
[14] F. Yang, J.R. Sambles. *J. Opt. Soc. Am.*, **B16**, 488–497 (1999).
[15] I. Hirosawa. *Jpn. J. Appl. Phys.*, **36**, 6953–6956 (1997).